UC San Diego

UC San Diego Previously Published Works

Title

Full-field Ultrasonic Data Analysis Based on Statistical Covariance Method

Permalink

https://escholarship.org/uc/item/3p50v9f4

Authors

CHONG, SEE YENN

TODD, MICHAEL D

Publication Date

2023-06-04

DOI

10.12783/shm2017/14115

Peer reviewed

eScholarship.org Powered by the California Digital Library
University of California

COVER SHEET

Title: Full-field ultrasonic data analysis based on statistical covariance method

Authors: See Yenn Chong
Michael D Todd

(FIRST PAGE OF ARTICLE)

ABSTRACT

Laser ultrasonic techniques (LUTs) are becoming widely used for damage detection based on full-field ultrasonic data. In general, LUTs provide three-dimensional (3-D) ultrasonic signals from which significant informative features may be extracted about the health condition of a structure. In this paper, statistical convariance method is proposed to investigate 3-D ultrasonic features. A laser ultrasonic interrogation method based on a Q-switched laser scanning system was used to interrogate 3-D ultrasonic signals in to a 2 mm aluminum plate. The ultrasonic signals in three-dimensional (3-D) space were generated, indexed by spatial N (*x*-direction), spatial M (*y*-direction), and temporal K (*t*-direction) samples, respectively. Then, two sets of covariance matrices were obtained based on the vector variables in *x*-direction and *y*-direction respectively for all *k* time samples respectively. The covariance imaging and the corresponding variance map were obtained. The wavelength and group velocity of S0 and A0 modes were able estimated from the variance map. The wavelength of the S0 and A0 modes were estimated with the deviation error of 2.3% and 11% respectively. The group velocities of S0 and A0 modes were estimated with the deviation error of 1.8% and 0.9%. The analysis will be further performed to develop group velocity curves for a range of frequency in metal and composite plates.

INTRODUCTION

Ultrasonic Lamb waves are well acknowledged in non-destructive evaluation (NDE) and structural health monitoring (SHM) applications because they can offer an effective method to estimate the location, severity and type of damage, as well as for long-range inspection of large structures. Lamb waves are dispersive and multimodal mechanical waves that propagate along a plate of relatively small thickness. The dispersive profile of Lamb waves may be obtained via representations in phase velocity curves and group velocity curves.

University of California San Diego, La Jolla, CA, 92093-0085, U.S.A..

In particular, group velocity curves are widely used for damage detection and localization by comparing the change of the group velocity between pristine and defective specimens. Ihn and Chang (1) measured and used group velocity to select Lamb wave S0 mode for the detection and monitoring of hidden fatigue crack growth in metallic structures based on damage index. Rosalie et al. (2) proposed to detect the change in group velocity of Lamb waves as the determinant parameter for the detection of delamination in GLARE aluminum plate-like structures. Ciampa and Meo (3) used the Lamb wave A0 mode group velocity to identify the location of acoustic emission (AE) sources due to low-velocity impacts in complex composite structures.

Many group velocity measurement methods are introduced to improve the accuracy of the damage detection and localization. One of the methods, time-of-flight (ToF) measurement, has long been used for group velocity estimation. Several ToF estimation methods, including cross-correlation, envelope moment, matching pursuit decomposition, and dispersion compensation, were studied and compared using a dispersive Lamb wave mode (4). Besides using ToF estimation methods, Draudvilienė and Mažeika (5, 6) proposed spectrum decomposition technique to development group velocity of Lamb waves in an aluminum plate. The method enables to reconstruct the dispersion curves of the fundamental modes with relative errors around 2%. Recently, Jarmer et al. (7) demonstrated using phased array beamforming method to estimate dispersion curves for both isotropic and anisotropic materials. Phase velocity was estimated by using a narrowband wavenumber beamforming technique, and group velocity was estimated by phase array beamforming that targeted specific modes.

Besides using conventional contact sensor piezoelectric transducer, laser ultrasonic techniques are showed the ability of group velocity estimation with promising results. Harb and Yuan (8) used LDV to derive the dispersion curves for A0 Lamb wave mode based on time-frequency analysis method to extract the arrival times at different center frequencies. The time instants of each peak in the time slice are stored, which are associated with arrival times of Lamb modes at the point of measurement. Lee et al. (9) used pulsed laser for generating full-field ToF map for stainless steel pipe wall-thinning detection. Chong et al. (10) developed statistical threshold estimation method to determine full-field ToF for pipe wall-thinning detection.

Since laser ultrasonic techniques provide high space resolution and large full-field ultrasonic data set in 3-D space-time domain, laser ultrasonic techniques obtain an ultrasonic data set from which informative features may be extracted about the health condition of a structure. In this paper, authors propose to use statistical convariance to investigate the ability of the proposed method to extract useful features to estimate group velocity of fundamental modes for NDE/SHM applications. In this paper, a full-field ultrasonic data of a 2 mm aluminum plate is interrogated and then the data with the center frequency of 400 kHz is processed to obtain the corresponding covariance matrix to generate covariance imaging. The variance values obtained in covariance imaging are evaluated for all time samples to determine the possible relationship between the theoretical group velocity and the variance signal in the variance map. Then, the features are extracted to estimate the wavelength and group velocity of the fundamental modes and compare to the theoretical group velocity.

FULL-FIELD ULTRASONIC DATA

Experimental Setup

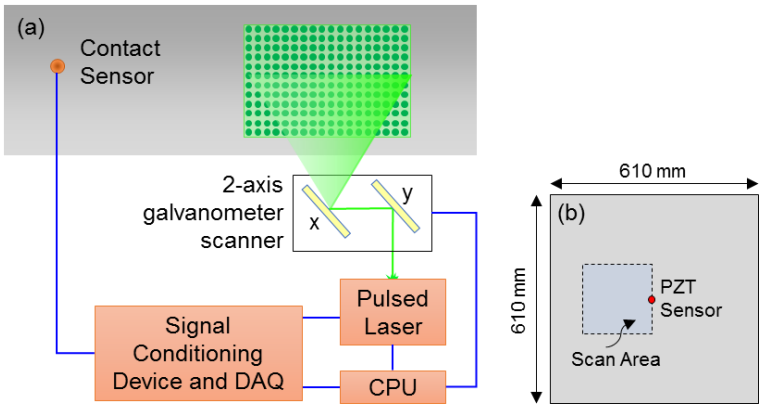

Figure 1. (a) Laser ultrasonic interrogation system configuration and (b) inspection configuration of a 2-mm aluminum plate.

Figure 1(a) shows a schematic diagram of a laser ultrasonic interrogation system, which consists of a laser scanning system incorporated with a signal conditioning device, a data acquisition (DAQ) module, a contact sensor, and a computer used for signal processing and operation control. The laser scanning system has a 2-D laser mirror scanner and a diode-pumped solid-state Q-switched Nd:YAG laser with 527 nm wavelength. In this paper, a 2-mm thick aluminum plate was setup at a stand-off-distance of 1780 mm from the 2-D laser mirror scanner. In Fig. 1(b), an area of 200 mm × 200 mm of the plate was scanned with a scan interval of 1 mm and a PZT sensor bonded at the center of the back-scan surface. The pulse repetition rate (PRR) was set to 20 Hz to avoid reverberation interference during the scanning process and the average energy was set to 1 mJ. The generated ultrasound was then signal-conditioned through the PZT sensor and digitized in the DAQ module as shown in Fig. 1(a). An in-line bandpass filter was used to filter ultrasonic signals at the center frequency of 400 kHz with the bandwidth of ±10 kHz. The DAQ module was set with a sampling time of T_S = 0.2 μs and K = 1000 total sample points. Once the scanning process was completed, the ultrasonic in 2-D space with N and M grid points on the target were generated and formed in a three-dimensional N by M by K space, indexed by spatial x-direction, spatial y-direction, and time, respectively, along each dimension as shown in Fig. 2(a).

CONVARIANCE MATRIX OF ULTRASONIC WAVEFIELD IMAGING

Covariance (as a linear dispersion estimator) is defined as the mean value of the product of the deviations of two variables from their respective means. When it comes to two-dimensional covariance problem, it may be expressed as a covariance matrix. For that, the convariance matrix of 2-D ultrasonic wavefield imaging at each time-frame k (Fig. 2(a)) is calculated. Since ultrasonic wavefield imaging at each time-frame k is formed in $N \times M$ matrix as shown in Fig. 2(a), the elements of the $N \times M$ matrix are ultrasonic amplitudes and grouped into two random vectors, column vector

$\mathbf{X}_m$ and row vector $\mathbf{Y}_n$ for X-axis and Y-axis, as shown in Figs. 2(b) and (c), respectively. Then, the covariance matrices of $\mathbf{X}_m$ and $\mathbf{Y}_n$ are obtained respectively.

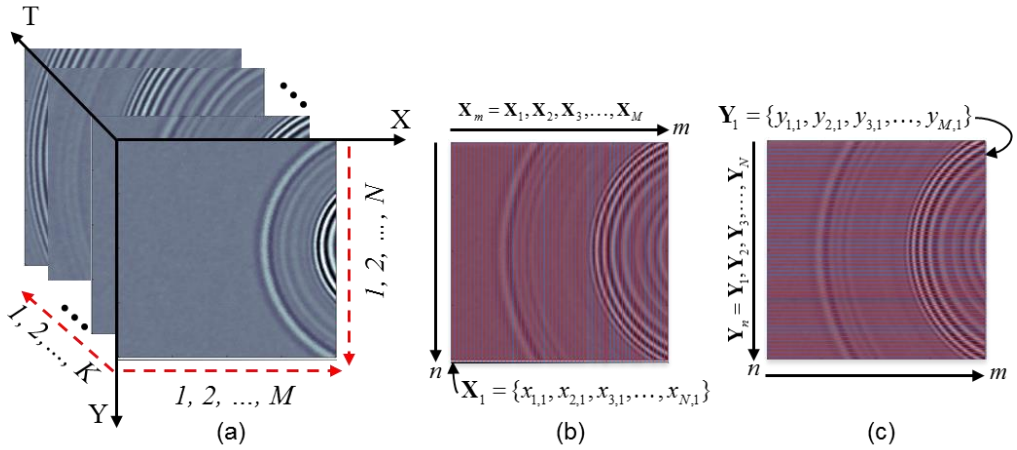

Figure 2. (a) Full-field ultrasonic data and convariance matrix notation for (b) *x*-axis and (c) *y*-axis at a discrete time *k*.

For the covariance matrix of $\mathbf{X}_m$, M column vectors are considered in the covariance matrix calculation. As shown in Fig. 2(b), $\mathbf{X}_m = \{x_{1,m}, x_{2,m}, \cdots, x_{N,m}\}$ is a column vector with a set of ultrasonic amplitude values (denoted as $x_{n,m}$) in spatial samples and n is an index that assigns a number to each spatial sample, ranging from 1 to N along Y-axis. The covariance matrix of $\mathbf{X}_m$ is denoted as $\mathbf{C}_\mathbf{X}$ and expressed below:

$$\mathbf{C}_\mathbf{X} = \begin{pmatrix} c_{1,1} & c_{1,2} & \cdots & c_{1,M} \\ c_{2,1} & c_{2,2} & \cdots & c_{2,M} \\ \vdots & \vdots & \ddots & \vdots \\ c_{M,1} & c_{M,2} & \cdots & c_{M,M} \end{pmatrix} \tag{1}$$

and the elements of $\mathbf{C}_\mathbf{X}$ are defined as:

$$c_{ij} = \frac{1}{N-1}\sum_{n=1}^{N}\left(x_{n,i} - \bar{X}_i\right)\left(x_{n,j} - \bar{X}_j\right) \tag{2}$$

and $i, j = 1, 2, \cdots, M$. $\bar{X}_i$ and $\bar{X}_j$ are the mean of each column vector $\mathbf{X}_m$. Since the covariance matrix in Eqn. (1) is a symmetric matrix with the matrix size of $M \times M$, for $i = j$ the diagonal elements, denoted as c_{ii}, contain the variances of column vector $\mathbf{X}_m$; and for $i \neq j$ the off-diagonal elements contain the covariance between all possible pairs of column vector $\mathbf{X}_m$.

As for the covariance matrix of $\mathbf{Y}_n$, the matrix $N \times M$ of the ultrasonic wavefield imaging (Fig. 2(a)) is transposed first. Then, $\mathbf{Y}_n^T = \{y_{n,1}, y_{n,2}, \cdots, y_{n,M}\}^T$ is obtained and used to obtained the covariance matrix of $\mathbf{Y}_n$ and the elements is defined as below:

$$c_{ij} = \frac{1}{M-1}\sum_{m=1}^{M}\left(y_{m,i} - \bar{y}_i\right)\left(y_{m,j} - \bar{y}_j\right) \tag{3}$$

and $i, j = 1, 2, \cdots, N$. $\mathbf{Y}_n^T = \{y_{1,n}, y_{2,n}, \cdots, y_{M,n}\}$ is a transposed $\mathbf{Y}_n$ with a set of ultrasonic amplitude values (denoted as $y_{m,n}$) in spatial samples and *m* is an index that assigns a number to each sample, ranging from 1 to *M* along X-axis. Since the covariance matrix is a symmetric matrix ($N \times N$), for $i = j$ the diagonal elements, denoted as c_{ii}, contain the variances of column vector $\mathbf{Y}_n$; and for $i \neq j$ the off-diagonal elements estimate the covariance between all possible pairs of column vector $\mathbf{Y}_n$.

RESULTS AND DISCUSSION

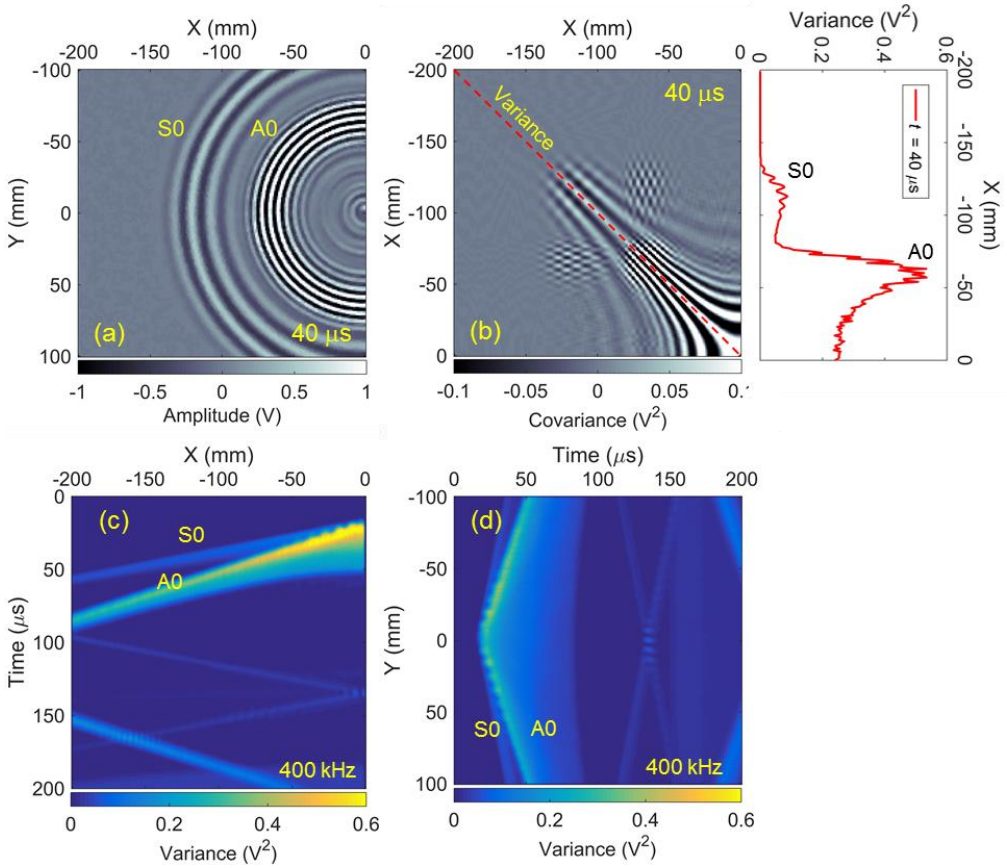

Figure 3. (a) Ultrasonic wavefield and (b) covariance images at 40 μs (insert: variance signal) for $\mathbf{X}_m$. Variance maps for the respective covariance matrices of (c) $\mathbf{X}_m$ and (d) $\mathbf{Y}_n$ with center frequency of 400 kHz.

Figures 3(a) and (b) show the ultrasonic wavefield and corresponding covariance images of $\mathbf{X}_m$ at the time of 40 μs. The Lamb waves, S0 and A0 modes, were clearly visible in the ultrasonic wavefield image. The diagonal of the matrix was the variances and the insert of Fig. 3(b) shows the variance signal in relative to the spatial sample points of X-axis. The variance signal showed multiple peaks along the two wave packets and the distance first arrival of the wave packets were similar to the distance first arrival of the S0 and A0 modes in ultrasonic wavefield (Fig. 3(a)). Figures 4(a) and (b) show the first arrival wavefronts of S0 and A0 modes in Fig. 3(a). Both wavelengths of the S0 and A0 modes were $\lambda_{AB} = \lambda_{A'B'} = 13\,\text{mm}$ and $\lambda_{CD} = \lambda_{C'D'} = 6$ mm as shown in Figs. 4(a) and (b). The deviation wavelength errors of the S0 and A0 modes between the wavelengths obtained in ultrasonic wavefield image (Fig. 3(a)) and in the theoretical calculation (Fig. 5(a)) are 2.3% and 11% respectively. Figures 4(c) and (d) show the zoomed variance signal of the insert of Fig. 3(b). The distances between the two peaks (AB and A′B′) of the variance signal in Fig. 4(c) were same as the wavelength of the S0 mode in Fig. 4(a). Both have the deviation wavelength errors of 9.8% (λ_{AB} = 12 mm) and 2.3 % ($\lambda_{A'B'}$ = 13 mm) in comparison with the theoretical wavelength. As for A0 mode, Figs. 4(d) shows the distances of λ_{CD} = 6 mm and $\lambda_{C'D'}$ = 6 mm with the deviation wavelength errors of (11%).

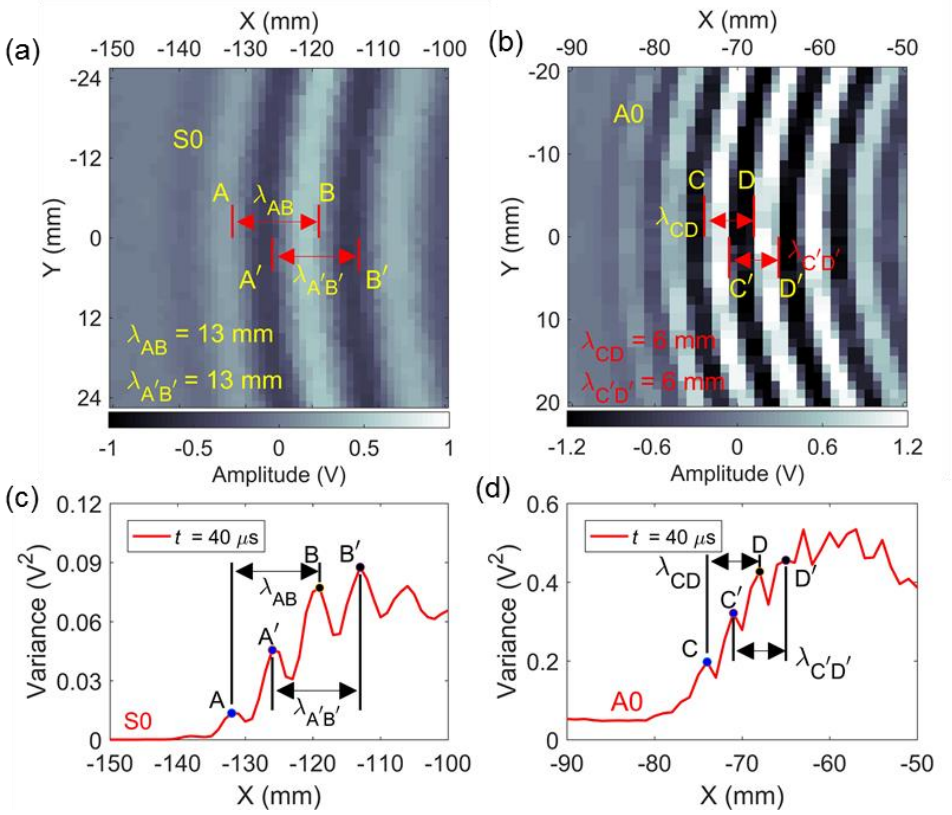

Figure 4. First arrival wavefronts of (a) S0 and (b) A0 modes and corresponding variance signals of (c) S0 and (d) A0 modes at 40 μs.

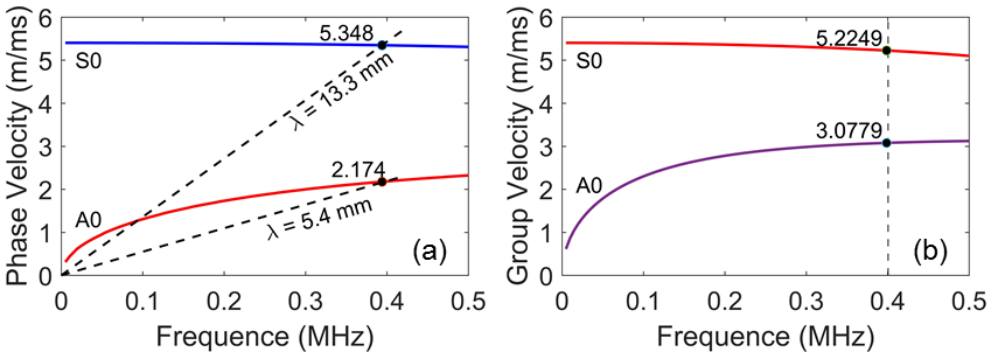

Figure 5. Theoretical (a) phase velocity curves and (b) group velocity curves of a 2 mm aluminum plate.

Since the wavelengths of S0 and A0 modes may be estimated from the multiple peaks in the variance signal, the variance signal may be further used to estimate the group velocities of S0 and A0 modes. For that, two variance signals at two different times in the variance map (Fig. 3(c) and (d)) can be used to estimate the group velocities. To calculate the group velocity for the right Lamb wave mode, the wavefronts of S0 and A0 modes must be separated as far as possible. With that, the variance map of $\mathbf{X}_m$ (Fig. 3(c)) was selected to estimate the group velocities of the S0 and A0 modes instead the variance map of $\mathbf{Y}_n$ (Fig. 3(d)).

Figure 6(a) shows two different variance signals at 35 μs and 51 μs. To calculate the group velocities of the modes, the same travelling wavefront (the peak of the variance signal) must be the same at two different times. Hence, the two peaks of A(–184, 0.02267) and A′(–99, 0.04462) for the variance signals at 35 μs and 51 μs were selected to determine the group velocity of the S0 mode as shown in Fig. 6(a). The distance ΔX_{S0} between the peaks at A and A′ was 45 mm and the group velocity of the S0 mode was 5.3125 m/ms. For the A0 mode, the two peaks of B(–106, 0.1678) and B′(–57, 0.3109) was selected with the distance ΔX_{A0} of 49 mm. Then, the group velocity of the A0 mode was 3.0625 m/ms.

In this paper, ten measurements of the full-field ultrasonic data at 400 kHz were obtained. Hence, the average group velocity of the S0 mode was equaled to 5.3188 m/ms with the deviation error of 1.8% to the theoretical group velocity of 5.2249 m/ms (Fig. 5(b)). Figure 6(b) show the ten measurements of peak A (–184 mm) and it shows that the repeatability was high where only the variance signal from one of the measurements (denoted P1) was diverse (a shaded circle in Fig. 6(b)) and the peak at –185 mm was selected instead –184 mm. For the A0 mode, the average group velocity of 3.050 m/ms with the deviation error of 0.9% to the theoretical group velocity of 3.0779 m/ms (Fig. 5(b)). The repeatability was high also but the same measurement P1 was different from the rest of measurements and the peak was shifted 2 mm as shown in the shaded circle in Fig. 6(c)).

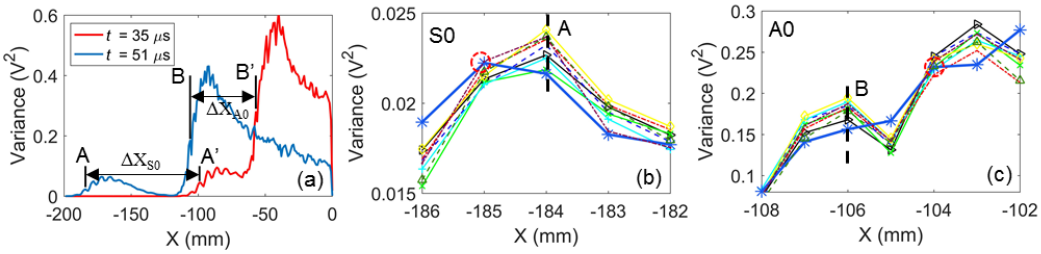

Figure 6. (a) Variance signals at 35 μs and 51 μs and ten measurements of the peaks at (b) A and (c) B.

CONCLUSION

In this paper, statistical covariance method was proposed, and it was demonstrated that the features of the variance map generated from the full-field ultrasonic data may be used to estimate the group velocities of Lamb wave fundamental modes. The full-field ultrasonic data of a 2 mm aluminum plate was obtained by a laser ultrasonic interrogation system incorporating with a Q-switched laser scanning system. Two covariance matrices of $\mathbf{X}_m$ and $\mathbf{Y}_n$ were obtained and represented in covariance images for all k time samples respectively. The variance signal obtained from the covariance images showed relationship to the S0 and A0 modes in the full-field ultrasonic imaging. The wavelength and group velocity of S0 and A0 modes were able estimated from the variance map. The wavelength of the S0 and A0 modes were estimated with the deviation error of 2.3% and 11% respectively. The group velocities of S0 and A0 modes were estimated with the deviation error of 1.8% and 0.9% respectively. Future works, the variance maps of a range of frequency will be generated to develop the group velocity curves for metal and composite structures. Then, the variance map will be investigated to seek for the possibility of using the map for damage visualization.

REFERENCES

1. Ihn, J.-B., Chang, F.-K. Detection and monitoring of hidden fatigue crack growth using a built-in piezoelectric sensor/actuator network: I. Diagnostics. Smart Materials and Structures. 2004;13(3):609.
2. Rosalie, S. C., Vaughan, M., Bremner, A., Chiu, W. K. Variation in the group velocity of Lamb waves as a tool for the detection of delamination in GLARE aluminium plate-like structures. Composite Structures. 2004;66(1–4):77-86.
3. Ciampa, F., Meo, M. A new algorithm for acoustic emission localization and flexural group velocity determination in anisotropic structures. Composites Part A: Applied Science and Manufacturing. 2010;41(12):1777-86.
4. Xu, B., Yu, L., Giurgiutiu, V. Advanced methods for time-of-flight estimation with application to Lamb wave structural health monitoring. 7th International Workshop on Structural Health Monitoring; 2009; Stanford University.
5. Draudvilienė, L., Mažeika, L. Measurement of the group velocity of Lamb waves in aluminium plate using spectrum decomposition technique. Ultragarsas" Ultrasound". 2011;66(4):34-8.

6. Draudvilienė, L., Mažeika, L. Investigation of the spectrum decomposition technique for estimation of the group velocity Lamb waves. Ultragarsas" Ultrasound". 2009;66(3):13-6.
7. Jarmer, G. J., Flynn, E. B., Todd, M. D. Dispersion curve estimation via phased array beamforming methods. Journal of Intelligent Material Systems and Structures. 2014;25(5):563-74.
8. Harb, M., Yuan, F. A rapid, fully non-contact, hybrid system for generating Lamb wave dispersion curves. Ultrasonics. 2015;61:62-70.
9. Lee, J.-R., Chong, S. Y., Jeong, H., Kong, C.-W. A time-of-flight mapping method for laser ultrasound guided in a pipe and its application to wall thinning visualization. NDT & E International. 2011;44(8):680-91.
10. Chong, S. Y., Lee, J.-R., Chan, Y. P. Statistical threshold determination method through noise map generation for two dimensional amplitude and time-of-flight mapping of guided waves. Journal of Sound and Vibration. 2013;332(5):1252-64.

DEStech Publications, Inc.

CONTRIBUTING AUTHOR COPYRIGHT RELEASE FORM

As author of the chapter/contribution titled Full-field ultrasonic data analysis based on statistical covariance method, to appear in the *Proceedings of Structural Health Monitoring 2017*, I hereby agree to the following:

1. To grant to DEStech Publications, Inc., 439 North Duke Street, Lancaster, PA, 17602, copyright of the above named chapter/contribution (for U.S. Government employees to the extent transferable), in print, electronic, and online formats. However, the undersigned reserve the following:
a. All proprietary rights other than copyright, such as patent rights.
b. The right to use all or part of this article in future works.

DEStech Publications thereby retains full and exclusive right to publish, market, and sell this material in any and all editions, in the English language or otherwise.

1 I warrant to DEStech Publications, Inc., that I am the (an) author of the above-named chapter/contribution and that I am the (a) copyright holder of the above-named chapter/contribution granted to DEStech Publications, Inc.

2 I warrant that, where necessary and required, I have obtained written permission for the use of any and all copyrighted materials used in the above-named chapter/contribution. I understand that I am responsible for all costs of gaining written permission for use of copyrighted materials.

3 I agree to assume full liability to DEStech Publications, Inc. and its licensee, and to hold DEStech Publications, Inc. harmless for any claim or suit filed against DEStech Publications, Inc. for violation of copyrighted material used in the above-named contribution.

Please sign and date this form and retain a copy for your records. Please include original form with your chapter/paper.

Thank you for your cooperation.

Please print name: Michael D Todd

Signed: _  _Dated: 05/15/2017

439 NORTH DUKE STREET • LANCASTER, PENNSYLVANIA 17602-4967, U.S.A. Toll Free: (866) 401-4337 • Tel: (717) 290-1660 • Fax: (717) 509-6100 E-mail: info@destechpub.com • Internet address: www.destechpub.com